

Near real-time input to an HF propagation model for nowcasting of HF communications with aircraft on polar routes

E.M. Warrington¹, A.J. Stocker¹, D.R. Siddle¹, J. Hallam¹, N.Y. Zaalov², F. Honary³, N.C. Rogers³, D.H. Boteler⁴ and D.W. Danskin⁴

¹ Department of Engineering, University of Leicester, Leicester, LE1 7RH, U.K.

² Department of Radio Physics, St. Petersburg State University, St. Petersburg, Russia

³ Department of Physics, Lancaster University, Lancaster LA1 4YB, U.K.

⁴ Natural Resources Canada, Ottawa, K1A 0Y3, Canada

ABSTRACT

The authors have previously reported on the development of an HF propagation model for signals reflected from the northerly regions of the ionosphere, and its validation by comparison with measurements made over a number of paths within the polar cap, crossing the auroral oval, and along the mid-latitude trough. The model incorporates various features (e.g. convecting patches of enhanced plasma density) of the polar ionosphere that are, in particular, responsible for off-great circle propagation and can lead to propagation at times and frequencies not expected from on-great circle propagation alone. Currently, the model drivers include ionosonde measurements and geomagnetic data from a period of several days spanning the time of interest. We have previously only examined the propagation effects on a historical basis, and have achieved good agreement between measurements and simulations.

There is a need for improved techniques for nowcasting and forecasting (over several hours) HF propagation at northerly latitudes to support airlines operating over the increasingly popular trans-polar routes. This is an area currently being addressed by the assimilation of real-time measurements into the propagation model, including ionosonde measurements to define the background ionosphere and Total Electron Content (TEC) measurements as indicators of the presence and magnitude of polar patches. The effects of D-region absorption in the polar cap and auroral regions is integrated in the model through satellite and ground-based measurements. The model development is supported by the collection of HF propagation measurements over several paths within the polar cap, crossing the auroral oval, and along the mid-latitude trough.

1 INTRODUCTION

Extensive HF propagation measurements have been made at northerly latitudes over a number of years by the University of Leicester and colleagues (see, e.g. *Warrington et al* [1997], *Zaalov et al* [2003], *Rogers et al* [1997; 2003], *Siddle et al* [2004a,b]). Of particular relevance to this paper, measurements undertaken in the polar cap found that the presence of convecting patches and sun-aligned arcs of enhanced electron density can lead to signals arriving in directions displaced from the great circle path by up to 100° [*Warrington et al*, 1997; *Zaalov et al*, 2003]. Patches are formed in the dayside auroral oval [see, e.g. *MacDougall and Jayachandran*, 2007] during periods of southward directed Interplanetary Magnetic Field (IMF) ($B_z < 0$) and the associated high levels of geomagnetic activity and generally convect in an anti-sunward direction across the polar cap into the nightside auroral oval, whereas arcs occur when geomagnetic activity is low and the IMF is directed northward ($B_z > 0$) and drift in a duskwards direction [*Buchau et al.*, 1983]. It was also found that the signals can arrive at the receiver over a range of directions with, for example, azimuthal standard deviations of up to 35° at frequencies of 2.8, 4.0 and 4.7 MHz being observed on one path from Isfjord, Svalbard to Alert, Canada [*Warrington*, 1998]. Similar measurements have also been undertaken at auroral latitudes [*Warrington et al*, 2006]. Although initially driven by direction finding interests, the measurements of direction of arrival undertaken in these experiments give insight into the complex propagation mechanisms present at high latitudes. It is particularly important to note that these propagation mechanisms have significant impact on the coverage of HF transmissions where the signals are reflected from the high latitude ionosphere.

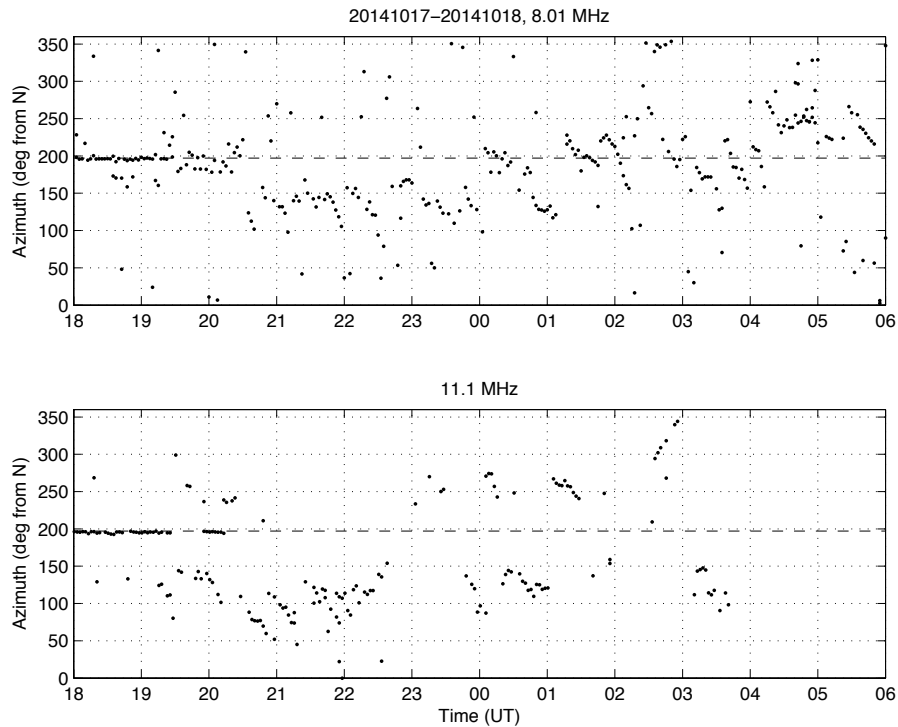


Figure 1. Measurements of direction of arrival of signals received over the Qaanaaq to Alert path at 8.0 and 11.1 MHz on 17-18 October 2014.

Example plots of the direction of arrival of 8.01 and 11.1 MHz signals received over the path from Qaanaaq, Greenland to Alert on 17/18 October 2014 are presented in Figure 1. It is evident from these data that the signals frequently arrive from directions well displaced from the great circle direction, at times without the presence of an on-great circle component. It is at times such as these that communications would be supported but not expected when only great circle propagation is considered.

2 CURRENT RAY-TRACING MODEL

We have previously reported on a ray-tracing model that can accurately reproduce many of the direction of arrival features observed in the experimental measurements [Zaalov *et al.*, 2003, 2005]. The simulations make use of the numerical ray tracing code developed by Jones and Stephenson [1975] to estimate the ray paths through a model ionosphere. Initially, a background ionospheric model is produced, which is then perturbed to include the various ionospheric features (in particular patches, arcs, auroral zone irregularities and the mid-latitude trough) that are expected to significantly affect the propagation of the radio.

Full details of the modelling are not included here, just some of the more pertinent points that are outlined below:

- The background ionosphere comprises two Chapman layers, the main parameters of which (critical frequency, critical height, vertical scale height of each layer) were determined from vertical ionospheric soundings. In view of the limited number of ionosondes available at high latitudes (and this number is decreasing), it was not possible to obtain snap-shots of the ionospheric parameters sufficient to define the background ionosphere. To overcome this difficulty, curves were fitted to the required parameters as a function of time for several ionosonde stations. These curves were then used as the basis of defining the latitudinal and longitudinal variation of the background ionosphere in terms of a series of spline fit curves, with longitudinal values obtained by rotating measurements along geomagnetic latitude with appropriate time shifts (up to ± 12 hours).

- Patches of enhanced electron density associated with high geomagnetic activity are modelled as an arbitrary number of Gaussian distributions with approximately equal longitudinal and latitudinal scale. The temporal evolution of the patches relative to the propagation path is simulated by means of a convection flow scheme coupled with the rotation of the Earth beneath the convection pattern, the precise form of which depends upon the components of the IMF [Lockwood, 1993].
- Sun-aligned arcs are defined within the model by a small number of three-dimensional Gaussian perturbations in electron density of different spatial scales (altitude, longitude and latitude) randomly distributed near to the centre of the arc. Several Gaussian perturbations are combined in defining the shape of each modelled arc in order to prevent the shapes of the arcs being too stylised.
- We employ an analytical approximation to the trough model presented by *Halcrow and Nisbet* [1977]. Their model is trapezoidal in form whereas our model has a smooth variation in electron density perturbation that is more physically realistic and is in a form suitable for ray tracing.
- The model also includes other features such as the plasma irregularities found in the auroral oval.

In addition to simulating the propagation of the HF radio waves, the effect of D-region absorption is also incorporated into the model. There are three principal mechanisms that are included: the diurnal absorption caused by solar uv [Davies, 1990], and the absorption that is associated with the X-ray flux and particle flux that results from a solar flare [Sauer and Wilkinson, 2008].

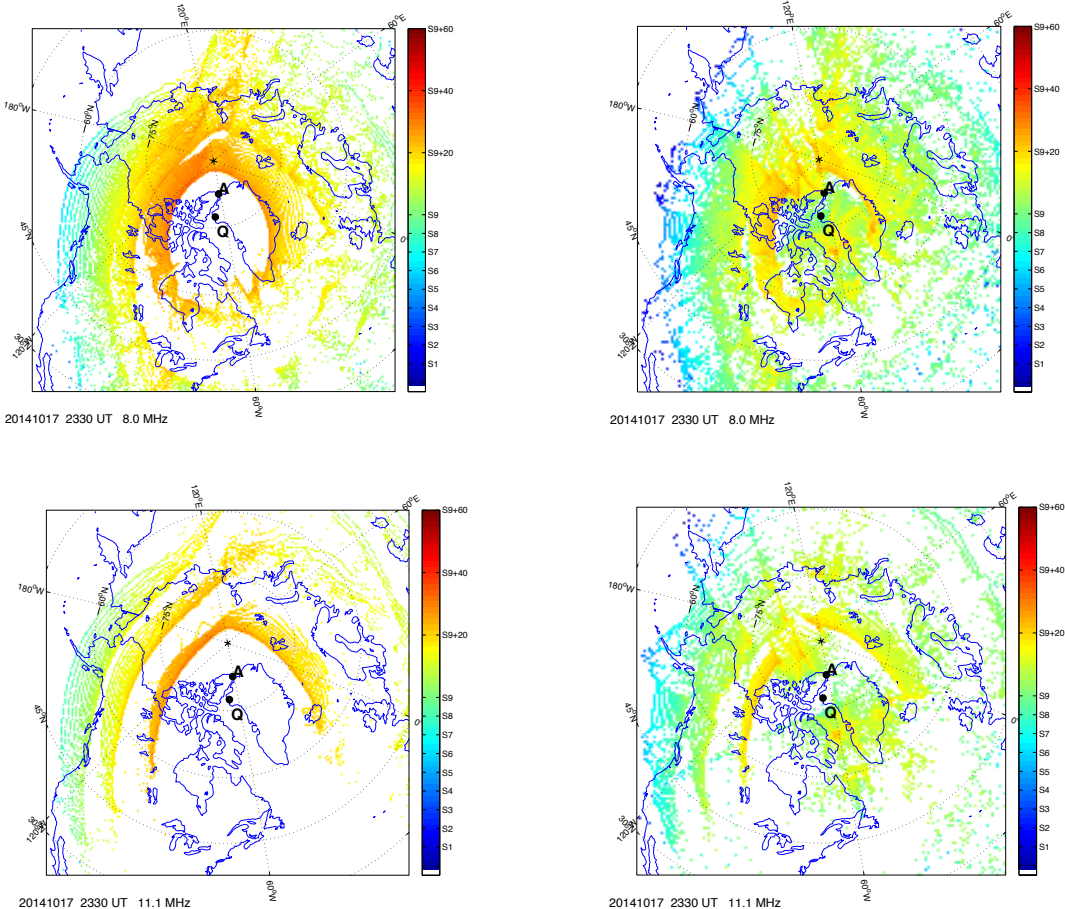


Figure 2. Predicted signal coverage at 8.0 and 11.1 MHz for a transmitter located in Qaanaaq. The left hand frames are for the background ionosphere, and the right hand frames for one particular patch scenario. The colours indicate the received signal strength while the position of the transmitter (Qaanaaq) and the receiver (Alert) are marked with Q and A, respectively.

The area coverage to be expected from a transmitter at a given location can then be estimated by ray-tracing through the model ionospheres. A large number of rays are launched in an azimuth / elevation grid from the transmitter. Each ray is assigned a power dependent upon the transmit antenna gain in the direction of the ray. The rays are then traced through the model ionosphere, adjusting the power as appropriate to take into account the D-region absorption, and the signal strength at the receiver estimated by adding the power conveyed by the rays to the receive antenna.

An example outcome of this modelling process is presented in Figure 2, where the received signal strength is estimated over the polar region for a transmitter located at Qaanaaq (Greenland) at frequencies of 8.0 and 11.1 MHz, corresponding to measurements presented in Figure 1. Taking just the background ionosphere into account, reception is not expected at Alert as it is within the skip zone at both frequencies. Including a set of randomly located patches significantly alters the ground coverage pattern, in particular resulting in signal coverage within the expected skip zone. In these cases, reflection has occurred from the patches rather than from the smooth background ionosphere and consequently the signal often arrives from directions offset from the great circle path, in agreement with Figure 1.

In considering the effect of the presence of patches, it is important to remember that in reality the patches will be distributed differently, will evolve in time, and will move generally following a convection pattern. To estimate the effect of patches on a statistical basis, a large number of simulations are undertaken, and the median and decile signal strengths calculated.

3 ONGOING DEVELOPMENTS TO THE RAY-TRACING MODEL

The methodology described in Section 2 has served us well in modelling specific historical events and investigating the effect of the presence of various ionospheric features, such as convecting patches of enhanced ionisation. Building the model though does require significant manual input, and is not directly readily adaptable to automated running, as is required in routine nowcasting and forecasting applications. We are currently developing the model for such applications using data that are available in near real-time.

The approach that we are currently adopting is to start with the IRI [Bilitza, 1990; Bilitza *et al.*, 2011] and to perturb this based on measurements made near to the time of interest to form the basis of the background ionosphere model employed in the ray-tracing procedures. This will then be further perturbed to include features such as the convecting patches, the parameters of which also be informed by measurements. One problem is the high variability of the high latitude ionosphere, and the relative scarcity of real-time measurements over the region.

Ionosonde measurements are perhaps the first to come to mind when considering HF propagation problems, and *Galkin et al.* [2012], for example, have considered integrating such measurements into a real-time IRI model. Whilst there are a significant number of ionosondes worldwide, coverage is not uniform, there are no instruments over the oceans, coverage (of particular relevance from the point of view of this paper) is sparse at high latitudes, and the number of ionosondes are decreasing with the possible exception of the Canadian CHAIN. Furthermore, high-latitude ionograms are not always easy to interpret, either manually or automatically. *Moskaleva and Zaalov* [2013] consider the signature of various high latitude ionospheric features on vertical ionograms. Two typical ionograms from Tromsø, Norway are given in Figure 3, the right hand frame corresponding to a time included in Figure 1 and the left hand frame to 12 hours earlier. As evidenced by this figure, at times it is relatively easy to obtain the required parameters (f_oF_2 , h_mF_2 , B_0 , ...) from the ionogram, whereas at other times the required features cannot be identified. Incorporation of oblique ionospheric soundings, perhaps incorporating directional information, will also form a valuable input.

A further source of ionospheric measurements that may be used is the IGS network of GPS receivers capable of measuring the total electron content along paths between individual receivers and individual satellites (this is referred to as the slant TEC, or sTEC). Many users have then converted the sTEC values into estimates of the vertical TEC (evTEC) making simplifying assumptions about the ionosphere, which we do not intend to do. Previous workers, for example *Komjathy et al.* [1998] and *Hernandez-Pajares et al.* [2002], have used GPS TEC measurements to update the IRI.

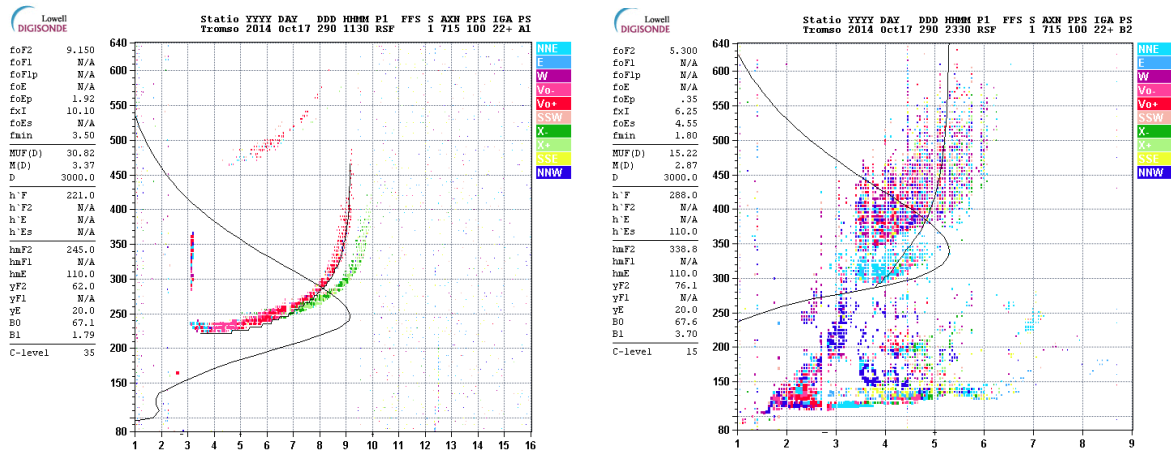


Figure 3. Ionograms from Tromsø on 17 October 2014. Left hand frame 11:30 UT and right hand frame 23:30 UT.

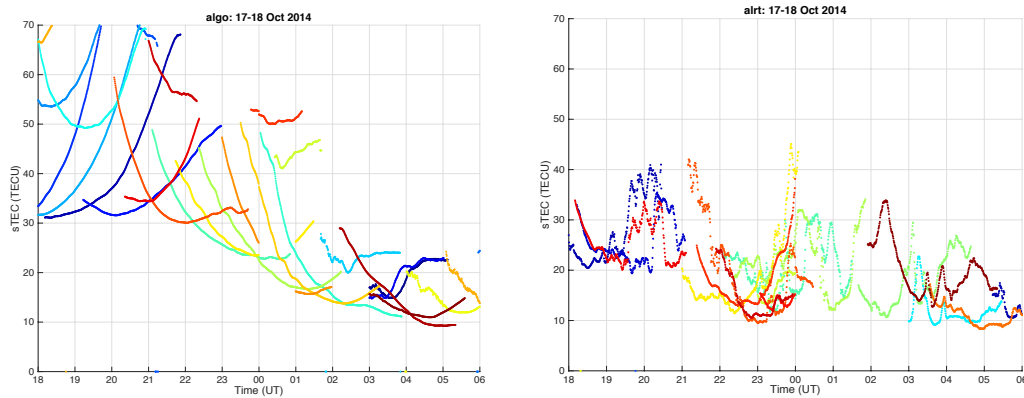


Figure 4. Slant TEC measurements made at Algonquin (left hand frame) and Alert (right hand frame) on 17-18 October 2014.

In addition to using GPS data to provide an estimate of the background ionosphere, it can also be used to establish the presence of patches, their location, and their intensity. However, there are limitations to this method since the GPS coverage is not complete and therefore patches might be present but not observed and therefore establishing the total number of patches is unlikely to be possible. However, the model can be run several times with different numbers of patches to give a range of possible outcomes.

Slant TEC (sTEC) measurements made at Alert with a number of GPS satellites at the same time as the measurements of Figure 1 are presented in Figure 4 alongside measurements made at a mid-latitude site at a similar longitude (Algonquin, Canada). The difference between the nature of the measurements made at the two sites is striking: at the mid-latitude site the traces are (more or less) smoothly varying, whereas at the high latitude site, significant deviations due to the presence of the patches is evident. Methods will need to be adopted that estimate the background sTEC curve from the measurements that have increased values due to the patches. It should also be possible to use these measurements to estimate the number of patches and their magnitude.

4 D-REGION ABSORPTION

Empirical models of HF absorption have been developed for the auroral regions [e.g. *Foppiano and Bradley, 1985*] and for the polar ionosphere during solar proton events [e.g. *Sauer and Wilkinson, 2008*]. Polar cap absorption (PCA) events may produce several dB of cosmic noise absorption, measured by riometers at 30 MHz, that can persist for several days [*Bailey et al., 1964*]. Over recent years, the number of riometers in the high latitude region has increased considerably, with 23 stations now operational in the Canadian region alone [*Danskin et al., 2008*], many of which are fitted with the capability of supplying near-real time (<15 minutes latency) measurements online. Consequently, new data-assimilative models have been developed in which the parameters of the PCA models are optimised in real time using a weighted non-linear regression to riometer measurements [*Rogers and Honary, 2015; Rogers et al., 2015*].

5 CONCLUDING REMARKS

A ray-tracing method has successfully been used to model the effects of the polar ionosphere on HF signals for historical scenarios. In order to apply this model to the nowcasting and forecasting of operational systems (e.g. the prediction of communications with commercial aircraft prior to dispatch) over a period of a few hours, we are currently incorporating data from a number of sources including ionosondes and GPS to provide real-time estimates of the background ionosphere and the number and intensity of patches. However, there are a number of challenges in this work that will need to be addressed.

- Small changes in the background electron density can lead to significant changes in the coverage particularly at distances close to the skip distance. Running the simulation several times with different versions of the background ionosphere and matching this to oblique measurements (such as the ones presented in Figure 1) will help address this.
- While ionosonde and TEC measurements will help establish the presence and intensity of patches, it is more difficult to determine the number of patches and their physical extent (since time and space are convolved in the GPS measurements because both the point where the path from the satellite to the ground intersects the ionosphere, the pierce point, and the patch are moving). However, we note that there will be some times when the same patch will affect the TEC on several GPS satellites (i.e. where the patch is larger than the separation of the pierce points), which will allow the size of a patch to be found. The simulation will be run with a range of different values of the patch parameters in order to establish an ensemble average of the coverage maps.
- The predictions are intended for relatively small disturbances where being able to use higher frequencies supported by off great-circle propagation and thereby avoiding the higher absorption at lower frequencies will provide a communication path. During periods of intense solar activity (e.g. where a large Coronal Mass Ejection impacts on the Earth), a complete absorption of HF signals is expected and hence at these times it is unlikely that successful communication in the polar cap will be possible.

ACKNOWLEDGEMENTS

The authors are grateful to the EPSRC for their support of this research through grants EP/K008781/1 and EP/K007971/1. We are also grateful to the University of Tromsø and the IGS for the ionograms and GPS data respectively downloaded from their internet sites and presented in this paper.

REFERENCES

- Bailey, D.K. (1964). Polar Cap Absorption. *Planet. Space Sci.* 12, 495-541, doi:10.1016/0032-0633(64)90040-6.
- Biliza, D. (ed.) (1990). *International Reference Ionosphere 1990*. NSSDC 90-22, Greenbelt, Maryland, USA.
- Bilitza, D., L-A McKinnell, Reinisch, B. and Fuller-Rowell, T. (2011). The international reference ionosphere today and in the future. *J. Geod.*, 85, 909-920, doi: 10.1007/s00190-010-0427-x.
- Buchau, J., Reinisch, B.W., Weber, E.J. and Moore, J.G. (1983). Structure and dynamics of the winter polar cap F region. *Radio Sci.*, 18, 995-1010, doi:10.1029/RS018i006p00995.

- Danskin, D.W., D. Boteler, E. Donovan and E. Spanswick (2008). The Canadian riometer array. *Proceedings of the 12th International Ionospheric Effects Symposium*, Alexandria, VA, USA, 13-15 May 2008, 80-86. (Available from www.ntis.gov, PB2008112709).
- Davies, K (1990). *Ionospheric Radio*. Peter Peregrinus Ltd on behalf of the IET.
- Foppiano, A.J. and P.A. Bradley (1985). Morphology of background auroral absorption. *J. Atmos. Terr. Phys.*, 47, 663–674, doi:10.1016/0021-9169(85)90102-3.
- Galkin, I.A., B.W. Reinisch, X. Huang and D. Bilitza (2012). Assimilation of GIRO data into a real-time IRI. *Radio Sci.*, 47, RS0L07, doi:10.1029/2011RS004952.
- Halcrow, B.W. and J.S. Nisbet (1977). A model of the F2 peak electron densities in the main trough region of the ionosphere. *Radio Sci.*, 12, 815-820, doi:10.1029/RS012i005p00815.
- Hernandez-Pajares, M., J. Juan, J. Sanz, and D. Bilitza (2002). Combining GPS measurements and IRI model values for space weather specification. *Adv. Space Res.*, 29(6), 949–958, doi:10.1016/S0273-1177(02)00051-0.
- Jones, R.M. and J.J. Stephenson (1975). *A Versatile Three-Dimensional Ray Tracing Computer Program for Radio Waves in the Ionosphere*. Office of Telecommunications, OT 75-76, U.S Department of Commerce, Washington, USA.
- Komjathy, A., R. Langley, and D. Bilitza (1998). Ingesting GPS-derived TEC DATA into the International Reference Ionosphere for single frequency radar altimeter ionospheric delay corrections. *Adv. Space Res.*, 22(6), 793–801, doi:10.1016/S0273-1177(98)00100-8.
- Lockwood, M. (1993). Modelling the high latitude ionosphere for time varying plasma convection. *Proceedings of the IEE*, part H, 140(2), 91-100.
- MacDougall, J., and P. T. Jayachandran (2007). Polar patches: Auroral zone precipitation effects. *J. Geophys. Res.*, 112, A05312, doi:10.1029/2006JA011930.
- Moskaleva, E.V., and N.Y. Zaalov (2013). Signature of polar cap inhomogeneities in vertical sounding data. *Radio Sci.*, 48, 547–563, doi:10.1002/rds.20060.
- Rogers N.C., E.M. Warrington and T.B. Jones (1997). Large HF bearing errors for propagation-paths tangential to the auroral oval. *IEE Proceedings on Microwaves Antennas and Propagation*, 14(2), 91-96, doi:10.1049/ip-map:19970663.
- Rogers, N.C., E.M. Warrington and T.B. Jones (2003). Oblique ionogram features associated with off-great-circle HF propagation at high and sub-auroral latitudes. *IEE Proceedings on Microwaves, Antennas and Propagation*, 150(4), 295-300, doi:10.1049/ip-map:20030552.
- Rogers, N.C., F. Honary, J. Hallam, A.J. Stocker, E.M. Warrington, D. Danskin and B. Jones (2015). Assimilative Real-time Models of HF Absorption at High Latitudes. *Proc. 14th International Ionospheric Effects Symposium*, Alexandria, VA, USA, 12-14 May 2015. (Available from www.ntis.gov).
- Rogers N.C. and F. Honary (2015). Assimilation of Real-time Riometer Measurements into Models of 1-30 MHz Polar Cap Absorption. *J. Space Weather and Space Climate*, doi:10.1051/swsc/2015009.
- Sauer, H.H. and D.C. Wilkinson (2008). Global mapping of ionospheric HF/VHF radio wave absorption due to solar energetic protons. *Space Weather*, 6, S12002, doi:10.1029/2008SW000399.
- Siddle, D.R., A.J. Stocker and E.M. Warrington (2004a). The time-of-flight and direction of arrival of HF radio signals received over a path along the mid-latitude trough: observations. *Radio Sci.*, 39, RS4008, doi: 10.1029/2004RS003049.
- Siddle, D.R., N.Y. Zaalov, A.J. Stocker and E.M. Warrington (2004b). The time-of-flight and direction of arrival of HF radio signals received over a path along the mid-latitude trough: theoretical considerations. *Radio Sci.*, 39, RS4009, doi: 10.1029/2004RS003052.
- Warrington, E.M., N.C. Rogers and T.B. Jones (1997). Large HF bearing errors for propagation paths contained within the polar cap. *IEE Proceedings on Microwaves, Antennas and Propagation*, 144(4), 241-249, doi: 10.1049/ip-map:19971187.
- Warrington, E.M. (1998). Observations of the directional characteristics of ionospherically propagated HF radio channel sounding signals over two high latitude paths. *IEE Proceedings on Microwaves, Antennas and Propagation*, 145(5), 379-385, doi:10.1049/ip-map:19982068.
- Warrington, E.M., A.J. Stocker and D.R. Siddle (2006). Measurement and modelling of HF channel directional spread characteristics for northerly paths. *Radio Sci.*, 41, RS2006, doi:10.1029/2005RS003294.

- Zaalov, N.Y., E.M. Warrington and A.J. Stocker (2003). The simulation of off-great circle HF propagation effects due to the presence of patches and arcs of enhanced electron density within the polar cap ionosphere. *Radio Sci.*, 38(3), 1052, doi:10.1029/2002RS002798.
- Zaalov, N.Y., E.M. Warrington and A.J. Stocker (2005). A ray-tracing model to account for off-great circle HF propagation over northerly paths. *Radio Sci.*, 40, RS4006, doi:10.1029/2004RS003183.